IEEE Access
Multidisciplinary | Rapid Review | Open Access Journal

Received February 13, 2018, accepted March 19, 2018, date of publication March 30, 2018, date of current version April 25, 2018.

Digital Object Identifier 10.1109/ACCESS.2018.2821196

On Chip Antenna Measurement: A Survey of Challenges and Recent Trends

M. RASHID KARIM[1], XIAODONG YANG[2], (Senior Member, IEEE), AND MUHAMMAD FARHAN SHAFIQUE[3], (Senior Member, IEEE)

[1]Department of Electrical Engineering, National University of Computer and Emerging Sciences, Islamabad 44000, Pakistan
[2]School of Electronic Engineering, Xidian University, Xi'an 710071, China
[3]Center for Advance Studies in Telecommunications, COMSATS Institute of Information Technology, Islamabad 45550, Pakistan

Corresponding authors: Xiaodong Yang (xdyang@xidian.edu.cn) and Muhammad Farhan Shafique (farhan.shafique@comsats.edu.pk)

This work was supported in part by the National Natural Science Foundation of China under Grant 61671349 and in part by the International Scientific and Technological Cooperation and Exchange Projects in Shaanxi Province under Grant 2017KW-005.

ABSTRACT Exponential increase in the requirements of cost effective and highly compact wireless modules has put system-on-chip (SoC) technology in high demand. On-chip-antenna (OCA) is an integral component of SoC-based wireless communication systems and has emerged as a perfect candidate for plethora of promising applications, especially at millimeter wave and terahertz frequencies. OCAs also support compact and low power applications of wireless sensor networks and Internet-of-Things. Since OCAs are manufactured on a single substrate along with other components, therefore their successful realization is subject to several challenges; the most significant of which is their accurate measurement. OCA's precise characterization is considered to be one of the toughest challenges to overcome since traditional off-chip antenna measurement setups are not suitable for this job. This calls for innovative measurement techniques, setups and solutions to enable their true characterization. Inspired by the significance of OCA characterization, this paper presents a comprehensive survey of the key recent developments in the field of OCA measurements. The techniques used to measure conventional off-chip antennas are briefly outlined followed by a succinct description of OCA's characterization challenges. The most recent trends and techniques of OCA measurement are expansively compiled. Some avenues for future trends in this regards are also delineated. It is anticipated that the presentation of this review will inspire the research community to come up with the novel methods and proposals to facilitate the OCA characterization process.

INDEX TERMS Antenna measurements, millimeter wave measurements, on chip antennas, system-on-chip.

I. INTRODUCTION

The world has witnessed an unprecedented advancement in the field of On Chip Antennas (OCA) in the last one decade owing to the creation of low cost, low power and miniaturized System-on-Chip (SoC) wireless communication systems. In comparison with conventional off-chip antennas, OCAs offer several advantages. Firstly, they reduce the size of the overall wireless communication system since there is no need of an impedance matching network between the antenna and RF front-end in the presence of an OCA [1]. Secondly, OCA based solutions offer high yield with greater repeatability, improved system bandwidth and straightforward system integration [2], [3]. Thirdly, OCA based wireless communication systems are power efficient since they do not dissipate large power in terms of dielectric losses and reflections [3], [4], [6], [7]. Finally, they provide flexibility to designers in the form of antenna and transceiver components co-design opportunity thus saving precious chip area and design time [2], [7].

OCAs are very promising for Millimeter Wave (MM-Wave) frequency applications since the size of an antenna element is essentially small at these frequencies and they produce lesser reflections as compared to that of a modular arrangement [8]. OCAs are equally favorable for Terahertz (THz) frequency applications owing to the availability of low cost Silicon based technologies; in this regards, a number of research works have already been reported [2], [8]–[13]. The examples of a few recently explored application areas of OCAs include; Inter and Intra-chip communication [14], electromagnetic energy harvesting [15], biomedical implant devices [16], [17], detection and imagining in THz region [18], Radio Frequency Identification (RFID)

based SoC [19], 3-D imaging [20], next generation wireless mobile terminal [21], measurement of MM-Wave ICs and devices [22], power combining [23], amplitude mono-pulsed radar [24], wireless system bandwidth enhancement [25] and beam steering [26].

Despite having multiple advantages and applications in several novel research domains, OCAs offer certain challenges as well, which need to be addressed judiciously. One of these is the degradation in their performance due to lossy Silicon substrate when designed in CMOS and SiGe-BiCMOS, which are the optimal technology choices for the modern SoC integration [8], [27]. The incompatibility of OCA's layout with technology process design rules is also very critical [6], [8]. In addition to that, the electromagnetic interaction with nearby passives is another fundamental problem related to OCAs [1], [28].

This review article is focused on the measurement challenges associated with OCAs. It also compiles a number of recent techniques proposed and successfully employed to characterize OCAs. The paper is organized as follows; section II summarizes the conventional off-chip antenna's measurement techniques. Third part of the paper delineates OCA measurement techniques that include measurement challenges and their solutions as proposed in different research works. Further research opportunities and future trends in this regard are proposed in the section IV.

II. MEASUREMENT TECHNIQUES FOR CONVENTIONAL OFF-CHIP ANTENNAS

Antenna measurement is an essential phase of an antenna design cycle. Antenna test ranges are used for measurements, where the Antenna-Under-Test (AUT) is characterized for its directivity, gain, polarization, impedance, current distribution and efficiency. These parameters are measured in the far-field of an antenna. The AUT can be used either as transmit or as receive antenna as suggested by the reciprocity theorem during the characterization process. For ease of measurements, the AUT is conventionally used as a receive antenna. Antenna test ranges are broadly classified into two categories; that are outdoor test range and indoor test range. Both of these types have certain limitations. Since outdoor test ranges are affected by environmental factors, they are prone to certain types of reflection errors. On the other hand indoor anechoic chambers are quieter in terms of reflections but they cannot accommodate large test structures such as ships or planes etc. Following common test ranges are used for characterizing different types of antennas, the details of these ranges are beyond the scope of this article.

- Ground reflection ranges
- Elevated ranges
- Slant ranges
- Compact antenna test range
- Near-field range

Interested readers may consult these references for further details on these test ranges [29], [30].

III. OCA MEASUREMENT: SIGNIFICANCE, CHALLENGES AND RECENT TRENDS

A. SIGNIFICANCE OF OCA CHARACTERIZATION

In comparison with other integrated components of SoC modules, the accurate characterization of an OCA is even more imperative, since a number of factors and error sources may affect its working that would ultimately lead towards poor performance of the module [31]. The detail of such factors and known error sources is discussed in the following subsections:

1) FABRICATION IMPREFECTION OF OCAS

Different kinds of error and defects may develop during the fabrication phase of OCAs. For example, the polishing stage of a finished chip may cause substrate thickness to change, which in turn may modify the OCA's impedance. Moreover, the polished surface may promote the generation and propagation of surface waves that can badly deteriorate OCA's performance [1]. Alternatively, the chip dicing process may create Residual Silicon Substrate (RSS) on the buffer area around an IC that can adversely affect OCA's characteristics as reported in [31], where 5 dB gain degradation happened as a result of RSS caused by the chip dicing process. This problem may get exacerbated when an OCA is integrated with other circuitry, as these circuits can act as RSS themselves for the OCA [31]. During the fabrication process, dimensions of an antenna chip may also change like in the case reported in [32], where the width of the OCA cavity varied during the fabrication process. Likewise in [33], a frequency offset of 1 GHz in reflection coefficient is observed due to variations in the patch length caused during the fabrication process. In addition, frequency shift of 4 GHz (from 10 GHz in simulations to 14 GHz in measurements) is observed in the OCA's reflection coefficient in [34] that is ascribed to the variations in substrate height and relative permittivity value post fabrication. The production tolerance is another critical factor that has to be essentially considered during OCAs measurement [35], since it is common for OCAs to vary a little during bulk production.

2) ERRORS CAUSED BY THE UNAVAILABILITY OF CO-SIMULATION DESIGN TOOLS

The unavailability of mutual Electronic Design Automation (EDA) tools, where OCA and other transceiver components can be designed and co-simulated, is another factor that makes OCA characterization crucial. OCAs are generally designed on electromagnetic simulation tools, whereas other transceiver components are designed on IC design packages. Antenna design tools do not have built-in functionality to perform the design rules check of an IC design process; as a result designers need to use IC design tools. Multiple iterations are often required between antenna simulators and IC design tools before the design is optimized; this leads towards longer design times and more efforts. OCAs require filling of dummy metal in their layout in order to comply

with the process design rules and to fulfill chip's stability requirements. Addition of dummy metal without proper simulations could result in serious post fabrication errors [5]. As an example, in [36], the simulation results of a 200 GHz fractal bowtie OCA demonstrate that the metal filled structure had badly affected its radiation patterns. Moreover, OCA simulations carried out on certain EDA tools are unable to include all attributes of a semiconductor process, thus making OCA characterization even more critical [37].

3) OTHER ERROR SOURCES

There are various other minor error sources that may contribute towards the performance deterioration of an OCA. The guard ring used around ICs to mitigate the substrate coupling effect can be one of such sources of deterioration. On the other hand, the problem of electromagnetic interference with on chip passives as well as the scattering from neighboring components may also degrade the impedance matching and radiation performance of an OCA [1], [32].

B. CHALLENGES IN OCA CHARACTERIZATION

OCAs cannot be measured with the conventional antenna measurement setups due to several restrictions enforced by those arrangements. Few of these limitations are elaborated in the following subsections:

1) FEEDING AND MOVEMENT LIMITATIONS

Traditional antenna measurement setups cannot accommodate the feeding and movement requirements of OCAs. For instance, instead of SMA or coaxial feeding, OCAs rely on tiny wafer probes which are connected to a transmission line or a waveguide structure though a holding arm. These accessories are not part of a conventional measurement setup thus lack in terms of the reconfigurability required for OCA measurement [38]–[40]. Moreover, in most of the conventional radiation pattern testing setups, the AUT rotates and the reference antenna is kept stationary; however, the rotation of an AUT is not trivial in OCA measurements due to the feeding mechanism limitations. Therefore, traditional measurement setups in their actual form are not suitable for the characterization of OCAs [5], [25].

Another common problem associated with OCA measurements is the precise alignment of probes with the feeding point of an OCA. The probes are aligned and skid precisely to make contact with the OCA. This alignment, especially with narrow pitch probes, requires a microscopic view of the feeding point and probes. Incorporating a microscope within the test chamber causes reflections that consequently affect the radiation pattern of the AUT. In addition to the alignment problems, Si wafers are also likely to get snapped during the process of wafer probing due to their fragile nature compared to orthodox PCBs, resulting into a permanent damage to the chip.

Embedded antennas for biomedical applications are gaining popularity in recent days where electrically small antennas are placed under skin at a certain part of human body.

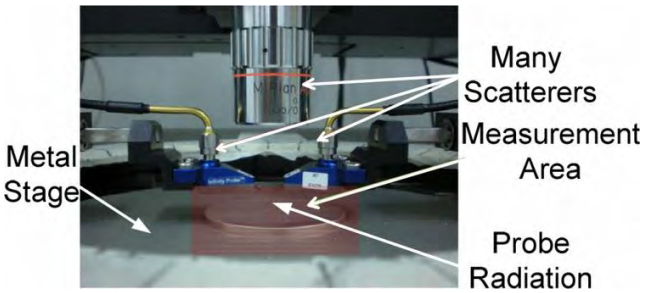

FIGURE 1. A typical probe station for an OCA characterization [41].

The characterization of these embedded antennas is also very challenging, since it is not possible to feed them directly with a coaxial probe therefore, a customized transition is generally required. These antennas have inherently low gain, thus adding transition further degrades their performance. Therefore, these effects must be compensated before taking measurements or during the post processing phase [41].

The OCA, fed with a probe setup, is illuminated by a standard gain horn antenna in the far-field during the measurement process. Instead of a 3 axis positioner of conventional measurement setups, this source horn antenna requires a modified rotating positioner which can rotate around the AUT. Similar problem arises with near-field scanning measurements where the near-field probe must rotate around the AUT to capture the radiating fields [42].

2) REFLECTION AND SCATTERING CAUSED BY PROBES AND OTHER METALLIC COMPONENTS

A typical probe station, for OCA measurement, comprises of different components as shown in Figure 1 [43]. Almost all components of the wafer probe station like chuck, microscope, positioner, probe table and probe tips are sources of reflections and scattering of electromagnetic fields that lead to erroneous measurement. It is difficult to avoid them since all metallic sections of a measurement setup cannot be covered with absorbers. During the measurement in commercially available probing stations, the chuck itself sometime acts as a ground plane and results in the generation of undesired modes. The back radiation from an AUT also gets reflected (Srefl) from the chuck and adds to the direct signal with a certain phase delay as shown in Figure 2a. Alongside, the radiation from the standard reference antenna may also get bounced between chuck and other metallic surfaces in the close proximity thus causing multiple reflections (Srefl1, Srefl2) as illustrated in Figure 2b [44].

While measuring an OCA using a standard wafer prober, the probes are placed closer to the AUT due to the compact size of the OCA; this arrangement contributes towards overall system noise and environment reflections which need to be minimized for correct characterization [35], [45]. A simple illustration of scattering phenomenon caused by a V-band probe is shown in Figure 3.

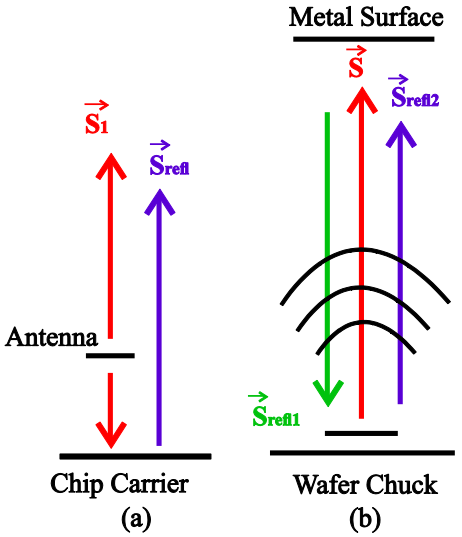

FIGURE 2. Metal chuck based reflections: (a) Back radiation from an AUT (b) Multiple reflections between the chuck and surrounding metallic surfaces [42].

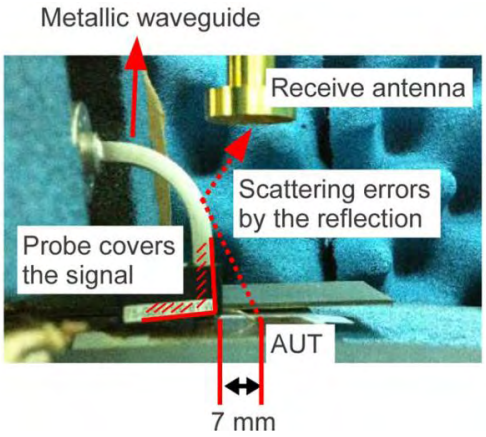

FIGURE 3. Illustration of scattering caused by a traditional V-band probe used for an OCA measurement [44].

3) UNDESIRED COUPLING EFFECTS CAUSED BY MEASUREMENT PROBES

The substrate residual current of an OCA may interact with the measurement probes thus producing errors in the measurements [47]. The unshielded tips of Air-Coplanar Probes (ACP) cause this coupling effect. The undesired coupling may also develop with the other structures like nearby passives etched on the same substrate as that of an OCA. The problem of unintended coupling cannot be compensated through the de-embedding process that is carried out with a calibration substrate [32]. This problem is investigated in [48] where an OCA was measured using Infinity®probes and ACP. The measurement results confirm the effects of undesired coupling through ACP which could not be removed even after de-embedding. As a result the resonant frequency was observed at 84 GHz instead of desired 77 GHz.

TABLE 1. Summary of OCA measurement problems.

Sr. No	OCA Measurement Problem	Significance
1	Need for replacement of x-y-z positioner with rotating positioner	• x-y-z positioner is not applicable for OCA
2	Movement restrictions of AUT	• The AUT and probe may get damaged if moved. • Requires movement of standard gain reference antenna which is not trivial.
3	Limited performance and low reconfigurability	• Leads to unreliable and nonrepeatable measurement results.
4	Metallic and unshielded measurement probes	• Causes reflection and scattering from the probes. • EM coupling / interference occurs. • Low gain OCAs are more challenging to measure. • Excites other passives on the chip in close proximity. • The de-embedding of probes fails to compensate the unwanted coupling effects.
5	Close proximity of the metallic chuck and reference antenna with the OCA during measurements	• Inability to use absorbers to cover the metallic chuck. • Becomes a major source of error due to reflection and scattering from standard antenna and chuck.
6	GSG pads produce capacitive effects mainly due to their injudicious placement in OCA layout.	• Shifts the resonant frequency and increase the return loss of an OCA.
7	Existence of substrate residual current in OCAs.	• Residual current interacts with measurement setup to cause uncertainty in measurements.

4) OTHER CHALLENGES

Ground Signal Ground (GSG) pads are made part of the OCA layout for measurement purposes. These pads introduce capacitive effects and consequently change the resonant frequency of the OCA. This is elaborated in [49] where the resonant frequency of the OCA is shifted from 77 GHz to 82 GHz and in [48] as well where an OCA resonates at 84 GHz instead of desired 77 GHz. In addition, location and placement of these pads may directly disturb the return loss characteristics of an OCA [49].

Table 1 summarizes the challenges associated with the probe based measurement setups. The accuracy and the reliability of measurements depend on the recognition and quantification of these error sources

C. RECENT OCA CHARACTERIZATION SOLUTIONS

Researcher have investigated rigorously to find optimum solutions to the challenges associated with OCAs in the last few years, and as an outcome a number of useful

measurement setups have emerged albeit with their own limitations. The majority of these measurement setups evolve from commercially available wafer probers where small modifications lead to improved OCA measurement by incorporating different off-the-shelf components [5]. The wafer probe based measurement setups employ Open-Ended Waveguide (OEWG) or horn as a standard reference antenna. OEWG is considered better as it does not require any probe compensation due to its low electric field interference with the AUT [5], [34]. Such measurement setups also use absorbers to mitigate the reflections caused by the probe with the nearby metals and its mounting structure [5].

The measurement techniques of OCA can be broadly characterized in to following two categories:

- Error compensation through pre/post-processing techniques
- Error compensation using modified measurement setup

1) ERROR COMPENSATION THROUGH PRE/POST PROCESSING TECHNIQUES

In this common technique, errors associated with the OCA measurement are mitigated with the help of pre or post-processing methods. Several such techniques have been proposed in recent literature, which are made part of this section. For OCAs, one of the fundamental challenges is to reduce the current on the substrate because it causes unwanted coupling with the nearby components and produces reflections during the measurement process. In [47], the inverse source technique has been used to compensate reflections from the nearby measurement equipment such as feeding cables and the mounting support. This reflection was caused by the coupling of substrate currents with the associated measurement equipment. A 60 GHz LTCC antenna has been measured using spherical near-field technique. During post-processing of the measured far-field data, the effects of the probes and the supporting equipment has been removed by spatial filtering of the undesired currents and the far-field pattern is produced from the current associated with the radiator only.

The behavior of ACP probe owing to large fringing fields has been discussed in section B. A simple yet effective method to de-embed the effects of an ACP probe has been proposed in [32]. The ACP probe used for measurements is modeled through software. The ABCD matrix of the probe is computed by simulation and its effect has been removed from the reflection coefficient of the actual measurements. Two W-band L and T shaped antennas have been measured for validation of this technique. The measurement has been carried out with a Vector Network Analyzer (VNA) along with VDI extenders. The reflection coefficients of these antennas, with and without de-embedding, are shown in Figure 4 and an improvement is noticeable in the case of de-embedded probes.

The identification of major reflection points in a measuring setup is highly desirable as this information can be used to correct the measured results by applying appropriate compensation techniques. Boehm and Waldschmidt [45] have

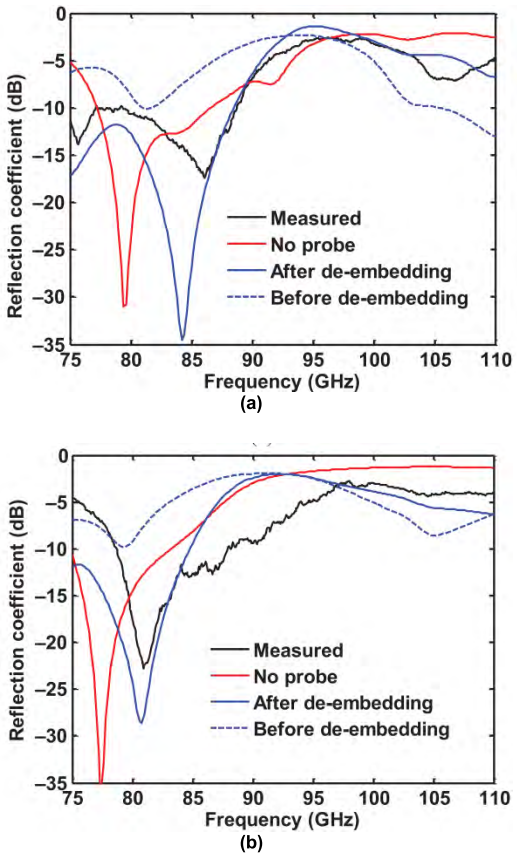

FIGURE 4. Reflection coefficients of W-band (a) T shape OCA (b) L shape OCA [30].

utilized two approaches to determine the main reflection points. They have used the far-field radiation pattern of an OCA at 160 GHz and applied extrapolation to the measured data. The radiation and gain results suggested that only those locations where ripples of the superimposed signal occur are beneficial for identifying the main reflection center. For accurate identification of the main reflection points, small distances from the AUT need to be considered only if the scattering happens close to the AUT, otherwise they can be ignored. By using this method, assessment and quantification of the measurement inconsistency and error have been successfully computed for OCAs operating at MM-Wave frequencies.

In [51], a post-processing technique of modal filtering is applied to minimize reflection from the OCA measurement setup at MM-Wave frequencies. The setup is based on a robotic control measurement system [38] that measured a 160 GHz OCA and later the proposed post-processing technique has been applied to the measured data. The impacts of limited scanning surface and flawed phase center position on the measurement results are also studied and a novel and robust method to determine the correct phase center is proposed. The application of this technique resulted in relatively less ripples in the measured radiation pattern. Moreover, this technique also facilitated to calculate the correct value of

directivity and makes it the first ever method to measure the directivity of an OCA with the help of a commercially available wafer prober at MM-Wave frequencies.

In order to address the errors associated with the reflections, researchers have proposed two methods based on superposition and S-parameters to compensate the scattering caused by the probe tips in [43]. In both methods, the radiations from the probe and the AUT are assumed to be superimposed at the receiving antenna; thus they are separated mathematically with the help of phasors created by the effects of probes only and the probe and AUT together. The first method uses only one probe and one AUT, but the second method needs two probes and two identical AUTs- positioned towards each other at a certain distance. The measurement results at 60 GHz for different OCAs conclude that the proposed methods are useful for low gain OCAs.

An efficacious effort has been made in [50] to identify different measurement error sources at MM-Wave frequencies. All measurements have been performed on a robotically controlled measurement setup and the effects of different error sources are noted on gain, directivity and radiation patterns of OCAs. The error sources investigated are related to the reference antenna, the measuring cables, and reflections from different parts of the setup, etc. In order to quantify the maximum deviation, the uncertainty budget for gain, directivity and radiation pattern has been computed and it was concluded that the main source of the uncertainty was reflections from the probes.

2) ERROR COMPENSATION THROUGH MODIFIED MEASUREMENT SETUP

The other major category in error compensation techniques is based on the modification of measurement setups in a judicious fashion. In one of such works reported in [44], a plastic chuck is designed and used, instead of a conventional metallic wafer chuck in order to reduce the reflections caused by metal parts in the setup. The measurements of a 278 GHz OCA using plastic chuck indicate significant reduction of ripples in the H-plane and the E-plane gain radiation patterns as compared to the measurements of the same OCA with the metallic chuck. This proves the effectiveness of the plastic chuck for the measurement of MM-Wave OCAs.

In [52], a measurement setup is proposed which has been evolved by mechanically modifying a conventional microelectronic probe measurement setup. Instead of a metallic chuck the proposed setup uses a special disturbance free foam holder to achieve metal free environment for measurements. The antenna gain using three gamma method, antenna efficiency, two and three dimensional radiation patterns and axial ratios of a few circularly polarized antennas have been measured using this setup. The reported accuracy of the setup is within $\pm$ 0.8 dB at 60 GHz.

In order to cater for undesired couplings caused by the proximity effects of an AUT and probes, a customized antenna measurement probe is designed for the measurement of OCA beyond 100 GHz in [35]. The probe has extended coaxial tip to increase the distance from the AUT as compared to that of a standard probe and thus reduces EM field interaction. The return loss, polarization, gain, radiation patterns and scattering centers, measured with the help of standard as well as custom made dedicated probe, of a 140 GHz OCA are compared. The results show considerably superior performance achieved by the customized probe, thus validating its use for measuring integrated antennas at MM-Wave.

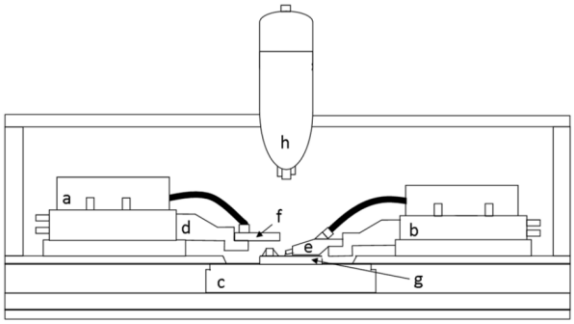

FIGURE 5. Measurement setup proposed in [40] where; a is MM-wave extension source, b is probe arm positioned, c is probe station platen, d is probe arm, e is GSG wafer probe, f is near-field scanning probe, g is AUT die and h is alignment microscope.

In a similar work proposed in [46], a measurement setup is designed to reduce the proximity effect. A custom made V-band probe is used that has modified fixture and extended probe tip feeder. The distance between the AUT and the standard receiving horn antenna has also been reduced for the calculation of near-field patterns. Verification of the proposed setup is conducted by measuring the return loss, radiation patterns and absolute gain of a 74 GHz OCA and results confirm the reduction of scattering waves. Easy integration of the proposed probe into a standard wafer prober and reduction of scattering and phase variations are the major advantages of this setup.

Generally near-field to far-field transformation is preferred over a direct far-field measurement in high frequency OCAs characterization due to space and measurement setup constraints. This approach also requires high precision moving stage and a suitable probe, which makes it necessary to carry out certain modification to the probing station. A suitable measurement setup for near-field scanning has been proposed in [42] where one of the probes is conventional GSG ACP probe connected to a VNA through a frequency extender, while the other ACP probe is replaced with a near-field scanner which is connected to the VNA's second port through another frequency extender. The setup is shown in Figure 5. Low reflections from the probing station and reduced cost and complexity are the main features of this setup.

In [5], a wafer prober based OCA characterization setup operable up to 67 GHz has been reported. The setup uses radiation absorbers, frequency extenders and OEWG as the probe antenna. Near to far-field transformation has been applied to measure radiation patterns in the far-field. The experimental results of a test horn antenna and a 2 $\times$ 2 patch antenna

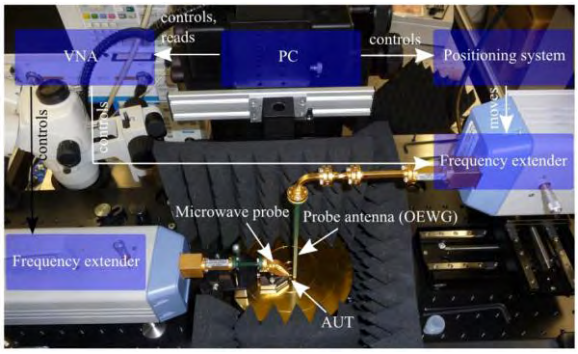

FIGURE 6. OCA characterisation setup proposed in [35].

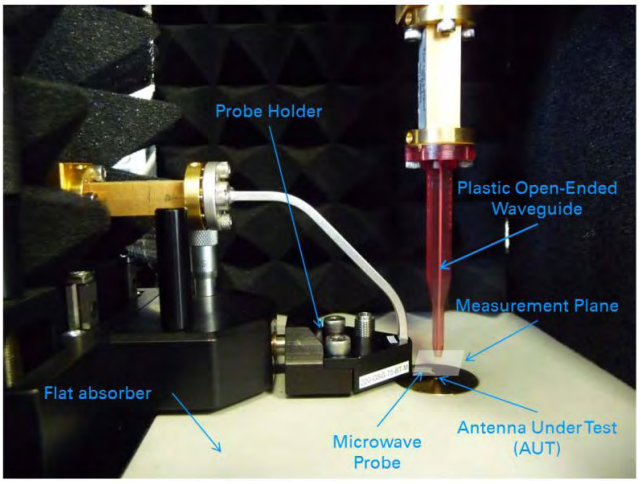

FIGURE 7. Measurement setup for 180 GHz OCA proposed in [25].

array show a little discrepancy in the measured E-plane and H-plane patterns, which is attributed to the reflections caused by the probe mounting. In [37], a similar measurement setup is presented which is capable of measuring radiation patterns up to 325 GHz. Frequency extenders (220 GHz to 325 GHz) have been utilized and a WR-3 twist has been installed between the OEWG and the frequency extenders to measure the second component of electric fields for the desired transformation (Figure 6). In the follow up of this work another study has been conducted in [36] where the same setup has been used to measure radiation patterns of four OCAs at 200 GHz. Only relative gain measurements have been reported due to unavailability of a calibration reference. The measured results of the normalized radiation pattern indicate agreement between simulated and measured results; but due to the absence of probe compensation, there is a slight difference between the two, especially towards the lower elevation angles.

In [25], a commercial wafer prober based measurement setup for 180 GHz OCA is proposed which utilizes near-field to far-field transformation and comprises of a VNA, frequency extenders, an OEWG and a computer (Figure 7). By moving the positioning stage, the probe antenna scans

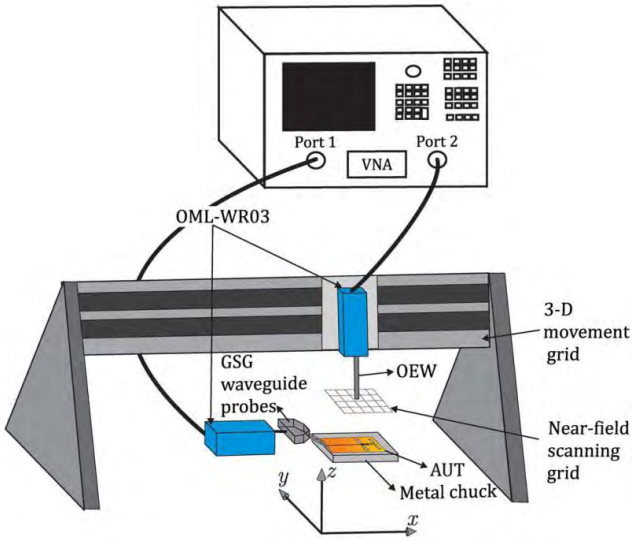

FIGURE 8. Near-field characterization schematic used in [51].

the measurement plane that hosts the AUT. For automated scanning, the stage is controlled by a computer. The proposed setup has two constrains; firstly it can only measure normalized gain; secondly, far-field measurement is only possible up to a critical angle which is contingent on the distance of an AUT from the measurement plane.

In [34], another wafer prober based radiation pattern measurement setup in the frequency range of 140 GHz to 220 GHz is demonstrated which utilizes near-field to far-field transformation and consists of a VNA, a special plastic OEWG receiving probe, frequency extenders, a 3-D AUT positioning system and a computer. A 180 GHz bowtie OCA is characterized with this setup and results show good agreement between simulated and measured response; however, only normalized gain is measurable with the proposed setup.

For radiation pattern measurements of a 0.3 THz OCA, a setup is designed in [53] (Figure 8) which utilizes near-field to far-field transformation technique. The setup uses commercial absorbers (ECCOSORB MMI-U) beneath OCA to suppress reflections. A standard probe correction method has been used to mitigate the effects of OEWG on OCA's far-field measurements. A good agreement in the H-plane radiation patterns is found. However, the E-plane patterns are oscillatory and nonsymmetrical owing to the interference caused by the probe radiations.

In [8], a setup for D-band (110 – 170 GHz) OCA characterization is proposed. The setup, shown in Figure 9a, employs a VNA, a MM-Wave controller, frequency extenders and 75 μm Infinity® D-band probes. The reference horn antenna rotates in semicircle to measure the radiation pattern. In order to reduce reflections, the AUT is mounted on a foam spacer with a low dielectric constant along with absorbers. Two standard 24 dBi horn antennas have been used with gain compensation technique to calibrate the measurement setup for the desired measurements. The measured results

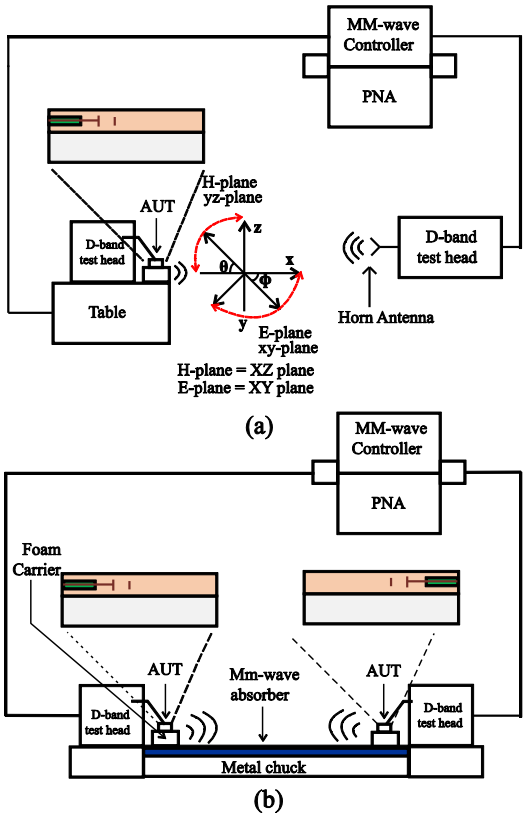

FIGURE 9. (a) Radiation pattern setup (b) Chip-to-chip communication based setup [8].

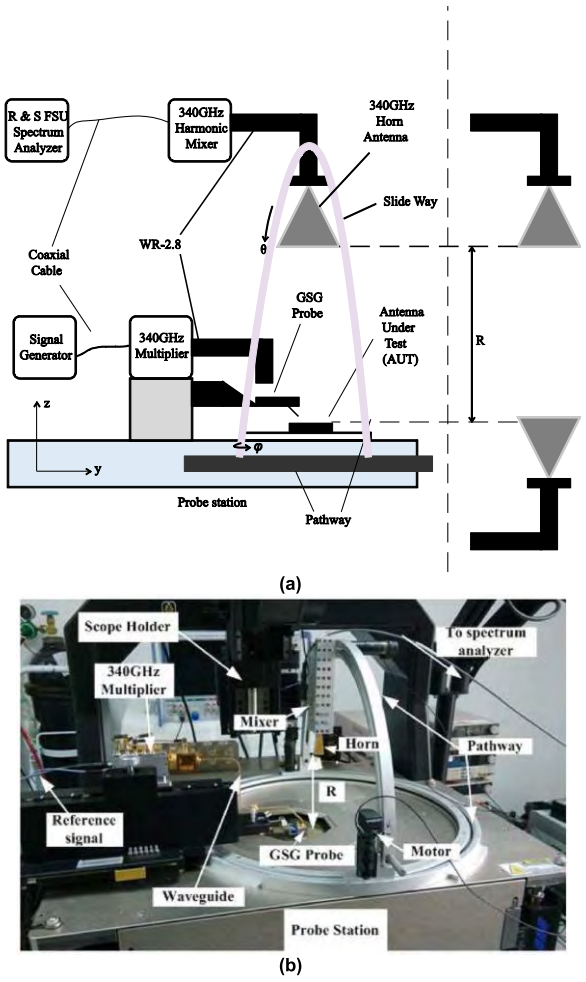

FIGURE 10. (a). Block diagram for gain and radiation pattern measurement setup (b) Photograph of measurement setup [2].

show good agreement with the simulated response. To verify it further, another chip-to-chip communication based measurement setup is established for the same OCA which is shown in Figure 9b. The antennas are kept at a distance of 10, 30 and 50 millimeters for the validation of Friis free space path loss. MM-Wave absorbers are also employed to mitigate reflections from the metal chuck. The efficiency of OCA is measured using the gain/directivity and Wheeler-cap method.

In [2], a 340 GHz 3-D yagi like OCA has been characterized for its gain and radiation pattern. The proposed setup, shown in Figure 10, consists of a signal generator, multipliers to generate 340 GHz signal, a 325 GHz waveguide-to-GSG probe, a 20 – 24 dBi gain standard horn antenna in 320 – 340 GHz range which is installed on a moving structure and kept at a far-field distance of 15 cm in the receiving path and a harmonic mixer. The measurements were performed by varying θ and ϕ angles. In order to measure gain, a reference setup, which comprizes of a short waveguide and a horn antenna, replaces the AUT and the GSG probes. The relation (1) has been used for peak gain measurement.

$$G_{peakAUT} = P_{AUT} - P_{HORN} + L_{PROBE} + G_{HORN} + L_{CABLE} \quad (1)$$

Where P represents received power, G is gain and L is loss with self-explanatory subscripts. Gain/directivity method is used for the efficiency measurement. The comparison of the simulated and measured gain shows a deviation of less than 1.5 dB; that is caused by the reflections from the metal probe station, probe holders and the slider way.

In order to measure Q-band OCA, a measurement setup (Figure 11) is presented in [54] which employs several absorbers to suppress the reflections from metallic parts of the system. The setup is based on a VNA and a spectrum analyzer. A standard horn antenna receives the signal transmitted by the AUT. Short-Open-Load (SOL) calibration has been performed on the feeding probe tip. The signal received by the standard horn antenna is measured on spectrum analyzer and the gain is calculated by the standard Friis transmission relation. The comparison of the simulated and measured results shows a good agreement, but the effects of the probe reflections and multipath could not be eliminated completely from the measured results.

In another similar work which is reported in [55], a standard wafer probe station based measurement setup for a 200 GHz OCA is designed. The setup comprises of frequency converter modules and 140 – 220 GHz range WR-5 waveguides. The calibration has been carried out using a standard

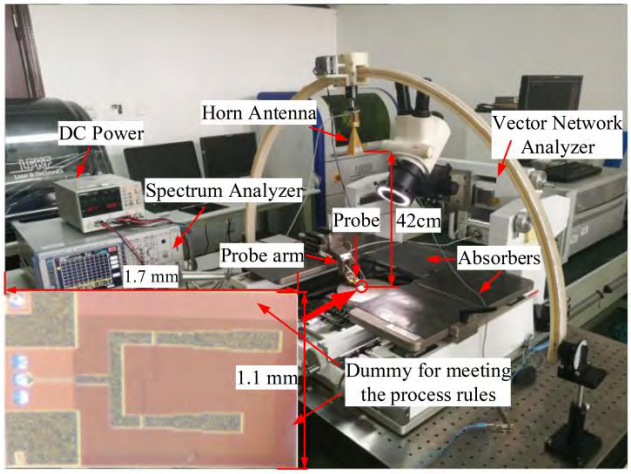

FIGURE 11. Q-band OCA characterization setup as proposed in [52].

calibration substrate. The setup offered errors due to mismatched properties of the calibration substrate as compared to the AUT substrate. Also, the close proximity impact of AUT and the probes along with multipath effects contribute to the reflections from the surrounding metallic objects.

In [56], a characterization setup to measure reflection coefficient and gain of a D-band OCA is proposed which consists of a VNA, 125 – 180 GHz frequency enhancement modules and absorbing materials (Figure 12). To calibrate VNA with the GSG probes, Line-reflect-match method has been used. For gain calculation two similar AUTs are placed at a specific distance in addition to the VNA and the frequency extenders. The AUTs have been fed by waveguide based GSG probes. The gain of the AUT has been calculated from the relation (2).

$$Gain\ (dBi) = \frac{[s_{21}\ (dB) - L_{fspl}(dB)]}{2} \tag{2}$$

Where L_{fspl} is the free space path loss for the AUT with separation of 2.5 cm. Due to assembly variations, simulated and measured gain differ within 1 dBi.

A setup for the measurement of a V-band OCA has been proposed in [6] (Figure 13). The OCA is glued to RT/Duroid 5880 low loss laminate prior to measurements. For reflection coefficient measurement, a VNA is used along with infinity® I-67 GSG probes. In order to measure gain, another setup has been established which is based on the gain transfer method and also includes an analog signal generator, a spectrum analyzer, a harmonic mixer and a WR-15 standard horn antenna. The AUT is excited by the signal generator and the transmitted power is captured by the standard gain horn antenna which is placed at a distance of 25 cm from the AUT. The signal is down converted by a mixer and passed on to the spectrum analyzer to check the power level. The measurement has been repeated for which the AUT has been replaced by the standard gain antenna. The two measurements, one with the standard antenna and another with the AUT, give relative gain of the AUT. A minor disagreement in reflection coefficient and gain

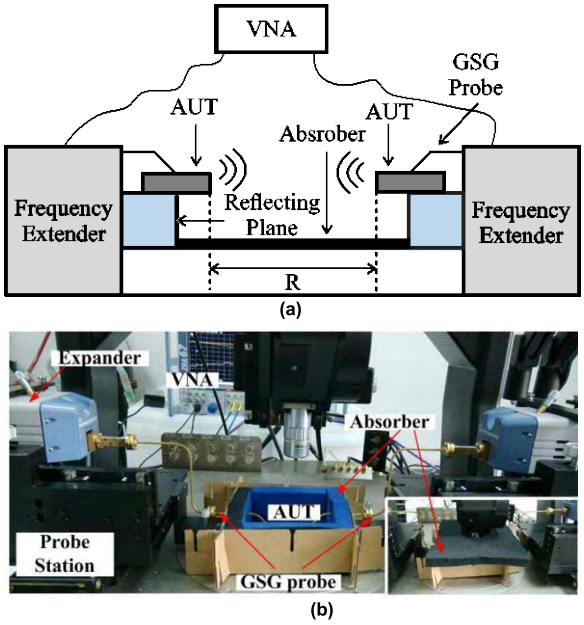

FIGURE 12. (a). Block diagram of the measurement setup for gain and reflection coefficient (b) Photo of actual measurement setup [54].

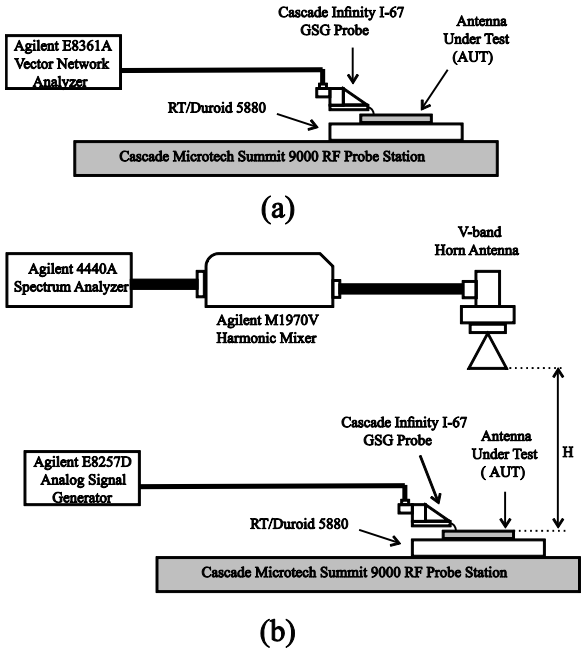

FIGURE 13. (a). Reflection coefficient measurement setup (b) Relative antenna gain setup [6].

between simulation and measured results are caused by the process variations and coupling between the antenna and the probe station.

In [57], an experimental setup to measure S-parameters and radiation patterns for a 60 GHz OCA is proposed (Figure 14). The S-parameter measurements are performed through Cascade probe station and a VNA. The reflection from metal chuck is controlled by mounting the sample onto a FR-4 board placed 3 cm away from the metal plate.

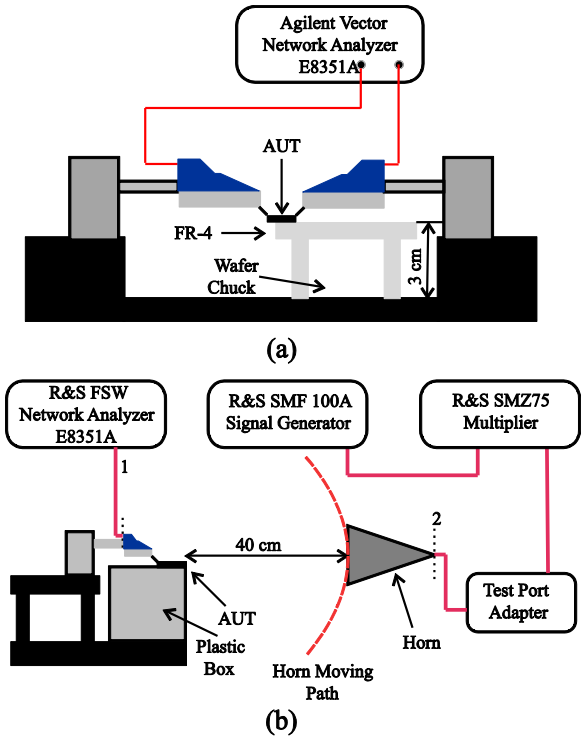

FIGURE 14. (a). Experimental setup to measure S parameters (b) Experimental setup to measure radiation pattern [55].

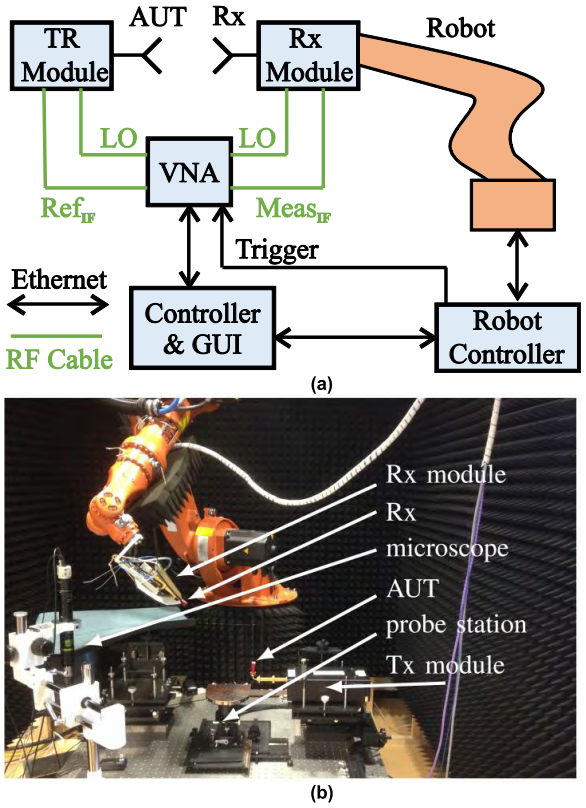

FIGURE 15. (a) Block diagram of the robotic setup [36] (b) Robot based measurement setup Photo [56].

For radiation pattern measurements, the metal chuck is replaced with a plastic box which supports the AUT and mitigates the unwanted reflections from the metallic parts of the setup. A mixer up converts the low frequency signal coming from the signal generator and feeds it to a standard horn antenna which launches it into free space. The AUT, placed at a distance of 40 cm from the horn antenna, receives the signal and sends it to the spectrum analyzer. The horn antenna moves in a circle to acquire the broadside radiation pattern. The peak gain is also calculated with the help of a relation which uses the signal power received at the spectrum analyzer.

Recently, another high-tech measurement setup has been proposed which is based on a robotic arm with six degrees of freedom as shown in Figure 15a [58]. The setup is reconfigurable, quick and is able to measure radiation pattern, gain, efficiency and other parameters of an OCA in the frequency range of 60 – 330 GHz. The robotic arm is attached to a computer and a VNA. Both, point-to-point and on-the-fly measurements are possible with the setup. The AUT transmits the signal that is captured by a standard gain horn antenna connected to the robotic arm. The computer controls the whole measurement process and the data is sent for post processing and far-field transformations. A 280 GHz OCA has been characterized using the proposed setup. Further discussion on this setup has been reported in [38] where the effects of calibration, dynamic range, absorber impact, etc. have been discussed. The photo of the setup is presented in Figure 15b. This setup is further enhanced in [40] by adding extra features such as the integration of a laser distance meter and the calculation of uncertainty budget for the measurement setup. The laser distance meter is utilized to find the accurate position of an AUT which then acts as an origin for the measurements. The gain, directivity and radiation pattern measurement of a 280 GHz horn antenna using this setup shows a good agreement with the simulation results. The slight discrepancy in the measured gain is associated with the attenuation in the connector. The setup supports the measurement in both near and far-field, as well as calculates the polarization of different types of OCAs.

In [49], a 77 GHz measurement setup to test reflection coefficient of OCAs is presented which consists of 110 GHz probes (ACP-110) along with a network analyzer (PNA-X 5245A). OCA is glued to a PCB to reduce reflections. In another research work a measurement setup for a 79 GHz OCA, integrated on a frequency modified constant wave radar chip, is demonstrated [33]. The broadside gain and return loss has been measured initially through feeding probes followed by the measurement of radiation pattern in an anechoic chamber. Through-Reflect-Line (TRL) calibration has been used to de-embed the probe tip with reference to the measurement plane. 1 GHz shift in the return loss has been observed primarily caused by the change in the length of patch during OCA fabrication process. A 20 dBi E-band horn antenna is mounted above the probe station chuck for a comparative gain measurement. The unshielded chuck causes

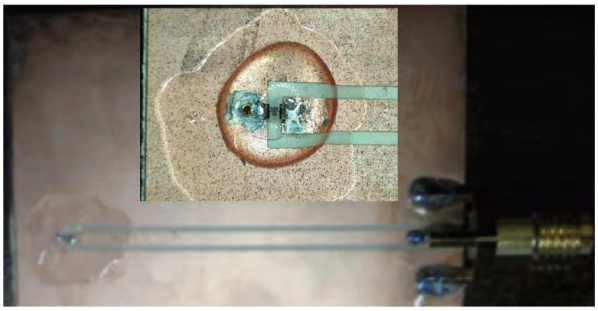

FIGURE 16. RF test structure with OCA chip connected [39].

ripples on the measurement curves due to multipath effect and 2 dBi gain degradation has been observed.

A methodology has been proposed to characterize embedded biomedical antennas in [41]. In these kinds of antennas the RF test board, transition between OCA and connector and the body phantom are the main sources of reflections which affect the antenna parameters. The researchers have modelled and calibrated all these error sources individually and combined through a simulator. The OCA has been mounted on a test board as shown in Figure 16 during measurements where signal is fed through a CPW line connected to the OCA. Various test boards with different CPW line configurations have been used. The results have been taken through a broadband horn antenna. It is stated that the prediction of reflection coefficient was possible with this methodology however the gain and radiation pattern was not measurable in this setup.

A comparative summary of measurement techniques discussed in this section is listed in table 2.

TABLE 2. Comparison of some recently proposed measurement setups.

S. No	Features	Limitations	Freq (GHz)	Ref.
1	Flexibility with respect to scan geometry, high resolution, point-to-point and on-the-fly (OTF) measurement support.	Reflections from probe station and robot, imprecise position of the robot and trigger for OTF measurement	60 – 330	[56]
2	Accurate, fast and reconfigurable, point-to-point and on-the-fly measurement support	Ripples over the frequency of interest which can be reduced with the use of an enhanced calibration method	60 – 330	[36]
3	Reduced wafer chuck reflections by the use of a plastic chuck. Less ripples in radiation pattern and gain. Substantial improvement in the measurement accuracy.	Special plastic chuck is required, modification in the measurement setup is necessary.	>100	[42]
4	Probe's scattering problem addressed. Lower EM interference in measured results as compared to a traditional probe	Around 0.37 dBi measurement gain deviation from that of simulations. Unmatched measured H plane radiation pattern.	>100	[33]
5	Controlled reflections from wafer chuck and probe, reduced scattering and phase variations	Custom probe requirement calls for the modified measurement setup.	V-band	[44]
6	Assessment and quantification of the measurement inconsistency and errors by finding the true scattering center.	Able to locate major reflection point only along the edge of the waveguide connector.	60 – 330	[43]
7	Quantification and approximation of different error sources which are part of the measurement setup. Estimation of the maximum deviation in results.	The directivity calculation is not possible in the lower hemisphere of the AUT Ripples in the measured results caused by the closed proximity of probe and AUT.	60 – 330	[48]
8	Reduced reflections in measured results, capable of determining directivity of MM-Wave OCAs using commercially available wafer probe	The reflection reduction algorithm is unable to rectify the reflection behind the probe.	60 – 330	[49]
10	Detection and suppression of unintended fields (residual current) due to OCA's interaction with the probe and other nearby components	Small ripples in radiation patterns are present due to the small residual current owing to close proximity of the antenna with the probe.	60	[45]
11	Analyzes effects of unshielded tips of ACP.	The measurement results are highly contingent on the antenna structure and the substrate used.	W – band	[30]

IV. FUTURE TRENDS IN OCAs

Since the demand for highly integrated, low power and cost effective wireless systems is tremendously growing, it is highly likely that OCAs will get more dominance in near future. To catch up with the escalating needs, researchers have to put in more efforts to propose innovative solutions in the domain of OCA realization and characterization. There are several auspicious domains in this regards, few of which are briefly discussed below:

A. MEASUREMENT SETUPS FOR MINIATURIZED OCAs FOR IoT BASED BIOMADICAL IMPLANTS

The most promising future application of OCA is in IoT wireless devices and systems which are expected to get dominance in near future [59]. A large proportion of IoT devices will be wireless [60] and they need to be compact, ultra-low power and in some cases battery-less. This set of requirements can be better achieved by designing these systems in Si based technologies and OCA can become part of these systems, thus making them more compact and cost effective. Remote health monitoring of patients is one of the most prominent applications of IoT [61] which may also include the use of

TABLE 2. ***Continued.*** **Comparison of some recently proposed measurement setups.**

12	Reduced reflection from the wafer probe station and chuck. Lower cost and complexity. Can be integrated with the commercial probe station	Customization of xyz positioner is necessary.	E – band	[40]
13	Characterization of electrically small OCAs for biomedical implants.	Unable to determine gain and radiation patterns. Test boards and body phantom affect the results.	1 – 8	[39]
	High measurement accuracy within ± 0.8 dB obtained through a metal free setup	No specific limitation reported	50 – 67	[50]
15	De-embedding of probe tips through TRL calibration to reduce effects on measurement results, On chip measurement of gain, return loss and radiation pattern are possible.	Ripples and 2 dB gain degradation has been observed.	75 – 84	[31]
16	Customized probe for controlled reflections	Ambiguity in the measured results regarding the position of null in the radiation pattern. .	140 – 220	[32]

biomedical implantable wireless devices [62]. Having said this, the use of OCA for such applications also offers certain challenges and accurate measurement is one of them. Already existing solutions are unable to measure implantable antennas as is the case discussed in [41], where reflection coefficient measurement was carried out but gain and radiation pattern could not be measured. Therefore, keeping the growing demands of embedded devices in mind, the gain and radiation pattern measurement is a potential future research area in OCA characterization.

B. MEASUREMENT OF ABSOLUTE GAIN AND DIRECTIVITY OF OCAs

Majority of the existing measurement setups are only capable of measuring normalized gain of an OCA since the reference measurements for absolute gain is not trivial. A possible future work is to enhance the capabilities of the existing setups and make them measure the absolute gain of OCAs. In existing literature there are a few setups which are capable of measuring directivity of OCAs at MM-Wave frequencies using commercially available wafer prober [51]. Further work in this regards is highly desirable.

C. CUSTOMIZED ANTENNAS WITH COLLIMATED RADIATIONS AND SMALLER APERTURE TO FACILITATE OCA MEASUREMENT IN FARFIELD

The most common approach in OCA measurements is near-to-far-field transformation; the motive for adopting this approach is tied to the room limitation for mounting the standard gain antenna. OEWG or conventional horn antenna is preferred which have a minimum far-field distance requirement. A research work can be beneficial in the area of compact antennas which can achieve closer far-field regions by either reducing the aperture or by converting the spherical waves into plane waves by special lenses or metamaterials. This will allow the measurement of radiation patterns in the far-field directly.

D. REDUCTION OF REFLECTIONS AND SCATTERING FROM THE MEASURING INSTRUMENT

Although quite a few innovative techniques have been proposed to eliminate reflections and scattering from the metallic wafer chuck and other instruments [35], [44] but still there is a huge research void in this area. It is always difficult to completely remove the coupling effects especially at high frequency while testing an OCA. It is envisioned that novel techniques either in the form of post processing or in the form of modified measurement setup is necessary for future generation of OCAs. The modification in the probe design could be beneficial in reducing couplings but the conversion loss should be kept under threshold which is a common trade-off when the conventional probe design is modified. A combination of post-processing techniques and modified measurement setup could be beneficial to reduce the reflections and scatterings from the measurement setup.

It is also important to ensure that the cost of modification in the setup remains in limits. In this regards the standard wafer probers are recommended as a basic building block.

E. MEASUREMENT SETUPS FOR 5-G MASSIVE MIMO OCAs

Massive Multiple Input Multiple Output (MIMO) is one of the key emerging technologies of the next generation networks i.e. 5-G which promises to bring benefits of spectrum efficiency, security, robustness, extremely low latency and power efficiency. To achieve these features, the front-end of 5-G enabled devices would rely on hundreds of antennas which will be operating simultaneously referred to as massive MIMO [63]. Miniaturization is the key to a successful implementation of 5-G mobile terminals and OCAs owing to their compactness are ideal candidate for these devices. A few OCAs for 5-G mobile terminal are already proposed in [21], [64], and [65]. However, no measurement setups for characterizing such OCAs is reported which makes it one of the attractive future research domains in OCAs.

V. CONCLUSION

In this paper, a thorough survey of the recent trends associated with OCAs characterization has been presented. The problems related to reflections from measurement equipment, EM interactions, movement limitations of the measurement setups and lack of required performance and reconfigurability of the setups are discussed in details. A number of recent techniques to overcome these problems have been compiled

which are categorized in the pre/post-processing techniques and the prudent modification of the existing measurement setup to overcome the measurement problems.

Furthermore, a concise description of a few future trends is provided with the anticipation that these will open up vast novel opportunities for research and explorations. In a nutshell, this paper is expected to provide an excellent platform to inspire the researchers to bring forward valuable solutions for OCAs characterization.

REFERENCES

[1] H. M. Cheema and A. Shamim, "The last barrier: On-chip antennas," *IEEE Microw. Mag.*, vol. 14, no. 1, pp. 79–91, Jan./Feb. 2013.

[2] X. D. Deng, Y. Li, C. Liu, W. Wu, and Y. Z. Xiong, "340 GHz on-chip 3-D antenna with 10 dBi gain and 80% radiation efficiency," *IEEE Trans THz Sci. Technol.*, vol. 5, no. 4, pp. 619–627, Jul. 2015.

[3] S. Yuan, A. Trasser, and H. Schumacher, "56 GHz bandwidth FMCW radar sensor with on-chip antennas in SiGe BiCMOS," in *Proc. Int. Microw. Symp.*, 2014, pp. 1–4.

[4] A. Barakat, A. Allam, H. Elsadek, H. Kanaya, and R. K. Pokharel, "Small size 60 GHz CMOS antenna-on-chip: Gain and efficiency enhancement using asymmetric artificial magnetic conductor," in *Proc. 44th Eur. Microw. Conf.*, 2014, pp. 104–107.

[5] B. Klein, M. Jenning, P. Seiler, K. Wolf, and D. Plettemeier, "Verification and demonstration up to 67 GHz of an on-chip antenna pattern measurement setup," in *Proc. IEEE Conf. Antenna Meas. Appl. (CAMA)*, Nov. 2014, pp. 1–4.

[6] C.-C. Liu and R. G. Rojas, "V-band integrated on-chip antenna implemented with a partially reflective surface in standard 0.13-μm BiCMOS technology," *IEEE Trans. Antennas Propag.*, vol. 64, no. 12, pp. 5102–5109, Dec. 2016.

[7] M. S. Khan, F. A. Tahir, and H. M. Cheema, "Design of bowtie-slot on-chip antenna backed with E-shaped FSS at 94 GHz," in *Proc. 10th Eur. Conf. Antennas Propag.*, 2016, pp. 1–3.

[8] W. T. Khan *et al.*, "A D-band micromachined end-fire antenna in 130-nm SiGe BiCMOS technology," *IEEE Trans. Antennas Propag.*, vol. 63, no. 6, pp. 2449–2459, Jun. 2015.

[9] A. Siligaris *et al.*, "A 278 GHz heterodyne receiver with on-chip antenna for THz imaging in 65 nm CMOS process," in *Proc. 41st Eur. Solid-State Circuits Conf.*, 2015, pp. 307–310.

[10] R. Wang *et al.*, "122 GHz patch antenna designs by using BCB above SiGeBiCMOS wafer process for system-on-chip applications," in *Proc. 24th Annu. Int. Symp. Pers., Indoor, Mobile Radio Commun.*, 2013, pp. 1392–1396.

[11] R. Song and Y. Li, "Simulation of on-chip antenna with resonant tunneling oscillator," in *Proc. Int. Microw. Workshop Ser. Adv. Mater. Process. RF THz Appl.*, 2016, pp. 1–3.

[12] M. G. Girma, J. Hasch, M. Gonser, Y. Sun, and T. Zwick, "122 GHz single-chip dual-channel SMD radar sensor with integrated antennas for distance and angle measurements," in *Proc. 44th Eur. Microw. Conf.*, 2014, pp. 1754–1757.

[13] J. Grzyb, K. Statnikov, N. Sarmah, and U. R. Pfeiffer, "A wideband 240 GHz lens-integrated circularly polarized on-chip annular slot antenna for a FMCW radar transceiver module in SiGe technology," in *Proc. Int. Microw. Optoelectron. Conf.*, 2015, pp. 1–4.

[14] D. Yi, L. Chong, H. Xiao-Wei, and T. Hong-Zhou, "12 GHz wireless clock delivery using on-chip antennas: A case for future intra/inter-chip wireless interconnect," in *Proc. Int. Conf. Comput. Sci. Autom. Eng.*, 2012, pp. 212–215.

[15] S. Yuxiang and A. Babakhani, "A wirelessly powered injection-locked oscillator with on-chip antennas in 180 nm SOI CMOS," in *Proc. Int. Microw. Symp.*, 2016, pp. 1–3.

[16] C. Liu, Y.-X. Guo, X. Liu, and S. Xiao, "An integrated on-chip implantable antenna in 0.18–μm CMOS technology for biomedical applications," *IEEE Trans. Antennas Propag.*, vol. 64, no. 3, pp. 1167–1172, Mar. 2016.

[17] F. Rodrigues, S. Gomes, P. Anacleto, J. Fernandes, and P. M. Mendes, "RF CMOS wireless implantable microsystem for sacral roots stimulation with on-chip antenna and far-field wireless powering," in *Proc. Eur. Microw. Conf.*, 2015, pp. 76–79.

[18] X. Lei-jun, T. Fu-cheng, B. Xue, and M. Han-Ping, "The design and matching of THz on-chip antenna in CMOS," in *Proc. Int. Conf. Microw. Millim. Wave Technol.*, 2016, pp. 958–960.

[19] S. Lischer, M. Heiss, M. Landwehr, and W.-J. Fischer, "A 24 GHz RFID system-on-a-chip with on-chip antenna, compatible to ISO 18000-6C/EPC C1G2," in *Proc. Int. Conf. Microw., Commun., Antennas Electron. Syst.*, 2015, pp. 1–4.

[20] P. Chen and A. Babakhani, "A 30 GHz impulse radiator with on-chip antennas for high-resolution 3D imaging," in *Proc. Radio Wireless Symp. (RWS)*, 2015, pp. 32–34.

[21] S. Sahin, N. K. Nahar, and K. Sertel, "On-chip UWB phased arrays for mmW connectivity," in *Proc. Int. Symp. Antennas Propag.*, 2016, pp. 1495–1496.

[22] C. Caglayan and K. Sertel, "On-chip 'baluntennas' for differential-mode noncontact characterization of mmW/THz devices and ICs," in *Proc. Int. Symp. Antennas Propag.*, 2016, pp. 249–250.

[23] B. Goettel, P. Pahl, C. Kutschker, S. Malz, U. R. Pfeiffer, and T. Zwick, "Active multiple feed on-chip antennas with efficient in-antenna power combining operating at 200–320 GHz," *IEEE Trans. Antennas Propag.*, vol. 65, no. 2, pp. 416–423, Feb. 2017.

[24] B. Goettel, J. Schaefer, H. Gulan, W. Winkler, and T. Zwick, "Double circularly polarized on-chip antenna for a 120–130 GHz amplitude monopulse radar," in *Proc. Eur. Radar Conf.*, 2016, pp. 409–412.

[25] R. Hahnel *et al.*, "Distributed on-chip antennas to increase system bandwidth at 180 GHz," in *Proc. German Microw. Conf.*, 2016, pp. 161–164.

[26] K. Sengupta and A. Hajimiri, "Mutual synchronization for power generation and beam-steering in CMOS with on-chip sense antennas near 200 GHz," *IEEE Trans. Microw. Theory Tech.*, vol. 63, no. 9, pp. 2867–2876, Sep. 2015.

[27] S. Pan, F. Caster, P. Heydari, and F. Capolino, "A 94-GHz extremely thin metasurface-based BiCMOS on-chip antenna," *IEEE Trans. Antennas Propag.*, vol. 62, no. 9, pp. 4439–4451, Sep. 2014.

[28] T. Deng and Y. P. Zhang, "On-chip antennas," in *Handbook of Antenna Technologies*, Z. N. Chen, Ed. Singapore: Springer, 2014, pp. 1–17.

[29] J. D. Kraus, R. J. Marhefka, and A. S. Khan, *Antennas and Wave Propagation*, 4th ed. New Delhi, India: McGraw-Hill, 2010.

[30] C. A. Balanis, *Antenna Theory Analysis and Design*. Hoboken, NJ, USA: Wiley, 2005.

[31] C.-C. Lin, C.-C. Chang, and S.-F. Chang, "The residual substrate effect in CMOS on-chip antenna," in *Proc. Int. Conf. Numer. Electromagn. Multiphys. Modeling Optim.*, 2016, pp. 1–2.

[32] M. Seyyedesfahlan and I. Tekin, "ACP probe measurement of on-chip strip dipole antennas at W band," *IEEE Trans. Antennas Propag.*, vol. 64, no. 4, pp. 1270–1278, Apr. 2016.

[33] M. Hitzler and C. Waldschmidt, "Design and characterization concepts of a broadband chip-integrated antenna," in *Proc. Eur. Microw. Conf.*, 2014, pp. 96–99.

[34] B. Klein, R. Hahnel, P. Seiler, M. Jenning, and D. Plettemeier, "On-chip antenna pattern measurement setup for 140 GHz to 220 GHz," in *Proc. Int. Conf. Ubiquitous Wireless Broadband*, 2015, pp. 1–5.

[35] L. Boehm, M. Hitzler, F. Roos, and C. Waldschmidt, "Probe influence on integrated antenna measurements at frequencies above 100 GHz," in *Proc. 46th Eur. Microw. Conf.*, 2016, pp. 552–555.

[36] M. Jenning, B. Klein, R. Hahnel, and D. Plettemeier, "On-chip integrated antennas for 200 GHz applications," in *Proc. Int. Conf. Ubiquitous Wireless Broadband*, 2015, pp. 1–5.

[37] B. Klein, M. Jenning, P. Seiler, K. Wolf, and D. Plettemeier, "On-chip antenna pattern measurement setup up to 325 GHz," in *Proc. Int. Symp. Antennas Propag. Conf.*, 2014, pp. 175–176.

[38] L. Boehm, S. Pledl, F. Boegelsack, M. Hitzler, and C. Waldschmidt, "Robotically controlled directivity and gain measurements of integrated antennas at 280 GHz," in *Proc. Eur. Microw. Conf.*, 2015, pp. 315–318.

[39] E. Lee, R. Soerens, E. Szpindor, and P. Iversen, "Challenges of 60 GHz on-chip antenna measurements," in *Proc. Int. Symp. Antennas Propag. USNC/URSI Nat. Radio Sci. Meeting*, 2015, pp. 1538–1539.

[40] L. Boehm, F. Boegelsack, M. Hitzler, and C. Waldschmidt, "The challenges of measuring integrated antennas at millimeter-wave frequencies [measurements corner]," *IEEE Antennas Propag. Mag.*, vol. 59, no. 4, pp. 84–92, Aug. 2017.

[41] H. Dinis, P. Anacleto, J. Fernandes, and P. M. Mendes, "Characterization of chip-size electrically-small antennas for smart wireless biomedical devices," in *Proc. 9th Eur. Conf. Antennas Propag.*, 2015, pp. 1–5.

[42] K. A. Ladds, H. P. Nel, and T. Stander, "A novel e-band nearfield scanner for wafer probed on-chip antenna characterisation," in *Proc. 10th Eur. Conf. Antennas Propag.*, 2016, pp. 1–4.

[43] J. Murdock, E. Ben-Dor, F. Gutierrez, and T. S. Rappaport, "Challenges and approaches to on-chip millimeter wave antenna pattern measurements," in *Proc. Int. Microw. Symp.*, 2011, pp. 1–4.

[44] L. Boehm, M. Hehl, and C. Waldschmidt, "Influence of the wafer chuck on integrated antenna measurements," in *Proc. German Microw. Conf.*, 2016, pp. 274–277.

[45] L. Boehm and C. Waldschmidt, "Scattering center determination for integrated antenna measurements at mm-wave frequencies," in *Proc. 11th Eur. Conf. Antennas Propag.*, 2017, pp. 1622–1625.

[46] Z. M. Tsai, Y. C. Wu, S. Y. Chen, T. Lee, and H. Wang, "A V-band on-wafer near-field antenna measurement system using an IC probe station," *IEEE Trans. Antennas Propag.*, vol. 61, no. 4, pp. 2058–2067, Apr. 2013.

[47] L. J. Foged, L. Scialacqua, P. Iversen, and E. Szpindor, "Detection and suppression of scattered fields from coplanar micro-probe and positioner in millimeter wave on-chip antenna measurements," in *Proc. Int. Symp. Antennas Propag.*, 2016, pp. 126–127.

[48] M. SeyyedEsfahlan and I. Tekin, "Radiation influence of ACP probe in S_{11} measurement," in *Proc. 10th Eur. Conf. Antennas Propag.*, 2016, pp. 1–4.

[49] M. SeyyedEsfahlan, M. Kaynak, B. Göttel, and I. Tekin, "SiGe process integrated on-chip dipole antenna on finite-size ground plane," *IEEE Antennas Wireless Propag. Lett.*, vol. 12, pp. 1260–1263, 2013.

[50] L. Boehm, F. Boegelsack, M. Hitzler, S. Wiehler, and C. Waldschmidt, "Accuracy evaluation for antenna measurements at mm-wave frequencies," in *Proc. 10th Eur. Conf. Antennas Propag.*, 2016, pp. 1–5.

[51] L. Boehm, A. Foerstner, M. Hitzler, and C. Waldschmidt, "Reflection reduction through modal filtering for integrated antenna measurements above 100 GHz," *IEEE Trans. Antennas Propag.*, vol. 65, no. 7, pp. 3712–3720, Jul. 2017.

[52] D. Titz, F. Ferrero, and C. Luxey, "Development of a millimeter-wave measurement setup and dedicated techniques to characterize the matching and radiation performance of probe-fed antennas [measurements corner]," *IEEE Antennas Propag. Mag.*, vol. 54, no. 4, pp. 188–203, Aug. 2012.

[53] W. H. Syed, G. Fiorentino, D. Cavallo, M. Spirito, P. M. Sarro, and A. Neto, "Design, fabrication, and measurements of a 0.3 THz on-chip double slot antenna enhanced by artificial dielectrics," *IEEE Trans. THz Sci. Technol.*, vol. 5, no. 2, pp. 288–298, Mar. 2015.

[54] Y. Song *et al.*, "An on-chip frequency-reconfigurable antenna for Q-band broadband applications," *IEEE Antennas Wireless Propag. Lett.*, vol. 16, pp. 2232–2235, 2017.

[55] P. Stärke, D. Fritsche, S. Schumann, C. Carta, and F. Ellinger, "High-efficiency wideband 3-D on-chip antennas for subterahertz applications demonstrated at 200 GHz," *IEEE Trans. THz Sci. Technol.*, vol. 7, no. 4, pp. 415–423, Jul. 2017.

[56] X.-D. Deng, Y. Li, H. Tang, W. Wu, and Y.-Z. Xiong, "Dielectric loaded endfire antennas using standard silicon technology," *IEEE Trans. Antennas Propag.*, vol. 65, no. 6, pp. 2797–2807, Jun. 2017.

[57] L. Jing, C. R. Rowell, S. Raju, M. Chan, R. D. Murch, and C. P. Yue, "Fabrication and measurement of millimeter-wave on-chip MIMO antenna for CMOS RFIC's," in *Proc. Int. Wireless Symp.*, 2016, pp. 1–4.

[58] L. Boehm, F. Boegelsack, M. Hitzler, and C. Waldschmidt, "An automated millimeter-wave antenna measurement setup using a robotic arm," in *Proc. Int. Symp. Antennas Propag. USNC/URSI Nat. Radio Sci. Meeting*, 2015, pp. 2109–2110.

[59] T. Schumacher, M. Stadelmayer, T. Faseth, and H. Pretl, "A review of ultra-low-power and low-cost transceiver design," in *Proc. Austrochip Workshop Microelectron. (Austrochip)*, 2017, pp. 29–34.

[60] Y. Qi *et al.*, "Review of the EMC aspects of Internet of Things," *IEEE Trans. Electromagn. Compat.*, to be published, doi: 10.1109/TEMC.2017.2775651.

[61] S. M. R. Islam, D. Kwak, M. H. Kabir, M. Hossain, and K.-S. Kwak, "The Internet of Things for health care: A comprehensive survey," *IEEE Access*, vol. 3, pp. 678–708, Jun. 2015.

[62] L. Wu, X. Du, M. Guizani, and A. Mohamed, "Access control schemes for implantable medical devices: A survey," *IEEE Internet Things J.*, vol. 4, pp. 1272–1283, 2017.

[63] A. Gupta and E. R. K. Jha, "A survey of 5G network: Architecture and emerging technologies," *IEEE Access*, vol. 3, pp. 1206–1232, Jul. 2015.

[64] J. Eisenbeis, F. Boes, B. Goettel, S. Malz, U. Pfeiffer, and T. Zwick, "30 Gbps wireless data transmission with fully integrated 240 GHz silicon based transmitter," in *Proc. IEEE 17th Topical Meeting Silicon Monolithic Integr. Circuits RF Syst. (SiRF)*, 2017, pp. 33–36.

[65] M. K. Hedayati, A. Abdipour, R. S. Shirazi, M. John, M. J. Ammann, and R. B. Staszewski, "A 38 GHz on-chip antenna in 28-nm CMOS using artificial magnetic conductor for 5G wireless systems," in *Proc. 4th Int. Conf. Millim.-Wave THZ Technol. (MMWaTT)*, 2016, pp. 29–32.

M. RASHID KARIM received the B.S. degree in telecommunication engineering from the National University of Computer and Emerging Sciences, Islamabad, Pakistan, in 2010, and the M.Sc. degree (Hons.) in microelectronics systems design from the University of Southampton, U.K., in 2012. He joined the Department of Electrical Engineering, National University of Computer and Emerging Sciences, in 2013, as a Lecturer, where he is currently an Assistant Professor. His research interests include integrated RF transceiver design, analog CMOS IC design, RF electronics, microwave & antenna design, and VLSI design.

XIAODONG YANG (SM'17) has authored or co-authored over 30 peer-reviewed papers in highly ranked journals. His research interests include body area networks, antennas and propagation, 5G, information security, wireless sensing, radar, millimeter wave technology, THz technology, nano communications, biomedical nano imaging, biomedical communications, visible light communications, calibration of vector network analyzer, machine learning, and so on. He has a global collaborative research network in the field of antennas and propagation, wireless communications, health informatics, information security, microwave techniques, and Internet of Things. He received the Young Scientist Award from the International Union of Radio Science in 2014. He is on the Editorial Board of several IEEE and IET journals, including the IEEE JOURNAL OF ELECTROMAGNETICS, RF AND MICROWAVE IN MEDICINE AND BIOLOGY, and so on.

MUHAMMAD FARHAN SHAFIQUE (S'08–M'11–SM'15) received the B.Eng. degree from Hamdard University, Karachi, Pakistan, in 2003, the M.S. degree from the University of Paris East Marne-La-Vallée, Paris, France, in 2005, and the Ph.D. degree in electronic and communications engineering from the University of Leeds, Leeds, U.K., in 2010. His research interests involve multilayer microwave device fabrication on LTCC technology, electromagnetic modeling of microwave structures, RF antenna, filters and MEMS packaging. He is also involved in dielectric characterization of materials using microwave techniques and fabrication of ceramic microfluidic devices. He is an Associate Director with the Center for Advanced Studies in Telecommunications, where he has established the Microwave Components and Devices Research Group. He has also setup a wide range of research facilities in the area of RF engineering which involves four state-of-the art laboratories. He is a reviewer of various journals.